Regular Article

A Method for the Tensile Strength Prediction of Tablets with Differing Powder Plasticities

Takeru Yano, Atsushi Oshiro, Shuji Ohsaki,* Hideya Nakamura, and Satoru Watano

Department of Chemical Engineering, Osaka Metropolitan University, 1–1 Gakuen-cho, Naka-ku, Sakai 599–8531, Japan.
*Correspondence: shuji.ohsaki@omu.ac.jp

Tablets are the most commonly used dosage form in the pharmaceutical industry, and their properties such as disintegration, dissolution, and portability are influenced by their strength. However, in industry, the mixing fraction of powders to obtain a tablet compact with sufficient strength is determined based on empirical rules. Therefore, a method for predicting tablet strength based on the properties of a single material is required. The objective of this study was to quantitatively evaluate the relationship between the compression properties and tablet strength of powder mixtures. The compression properties of the powder mixtures with different plasticities were evaluated based on the force-displacement curves obtained from the powder compression tests. Heckel and compression energy analyses were performed to evaluate compression properties. During the compression energy analysis, the ratio of plastic deformation energy to elastic deformation energy (E_p/E_e) was assumed to be the plastic deformability of the powder. The quantitative relationship between the compression properties and tensile strength of the tablets was investigated. Based on the obtained relationship and the compression properties of a single material, a prediction equation was put forward for the compression properties of the powder mixture. Subsequently, a correlation equation for tablet strength was proposed by combining the values of K and E_p/E_e obtained from the Heckel and compression energy analyses, respectively. Finally, by substituting the compression properties of the single material and the mass fraction of the plastic material into the proposed equation, the tablet strength of the powder mixture with different plastic deformabilities was predicted.

Key words   powder compression, tablet strength, elastoplastic mixture, heckel analysis, compression energy analysis

Introduction

Powder compression is the molding process for tablets during which pressure is directly applied to the powders. It has been utilized in various industries, including pharmaceuticals, ceramics, metals, batteries, and foods, because of its simplicity and low-cost mass production.[1–6] Particle properties such as shape, size, Young's modulus, and plastic deformability affect compact properties such as tablet strength and void fraction.[7–9] Tablet strength is a significant physical attribute because it strongly affects other important tablet properties, such as disintegration, dissolution, and portability. However, in industry, empirical-rule-based trial and error techniques are used to determine the mixing ratio of components, which strongly affects tablet strength. Therefore, a method for predicting tablet strength based on the properties of a single material is required. Tablet strength is related to the bonding properties between particles, such as the average coordination number of particles and plastic deformation. The relationship between the remaining strain and the tablet strength is often considered through numerical analyses using the finite element method.[10,11] The compression process induces significant densification of the powder bed owing to particle rearrangement and deformation. High compression pressure increases both the coordination number and contact area between the

particles.[12] Although the plastic deformability of individual materials has been evaluated, studies focusing on the plastic deformability of mixed powders and quantitative evaluation methods are insufficient.

Powder compression involves the following four processes: packing, compression, decompression, and ejection.[13–17] Because tablet strength is affected by the coordination number and contact area between particles during compression, powder compression behavior analysis is important.[18,19] A method for predicting the capping tendency was proposed based on the ratio of elastic to plastic energy obtained from compression energy analysis.[20] Measurement of the die wall pressure was also useful for estimating the capping tendency.[21,22] Four elementary processes occur simultaneously during powder compaction: rearrangement, elastic and plastic deformations, and brittle fracture.[23–27] Particle rearrangement is a phenomenon during which compression causes particles to move to a stable position without deformation, thereby increasing their coordination numbers.[28] X-ray microtomography of the compression process of the cohesive nanoparticles revealed that the density distribution in the powder bed during packing becomes uniform after compression.[29] Particle deformation can be divided into elastic and plastic deformation. During elastic deformation, the particle returns to its initial shape

after unloading, whereas plastic deformation is permanent. The deformation of the powder beds and the plasticity depend on the material characteristics. As high pressure is applied to the powder beds, the powder bed undergoes densification through brittle particle fracture caused by the compressive force. These elementary steps occur simultaneously and are influenced by the powder properties.[30] In addition, powder properties such as particle shape, size distribution, cohesiveness, Young's modulus, and plasticity significantly affect the structure of the compacts.[31,32]

Particle plasticity strongly affects the compression properties. Several models have been proposed to describe the plastic deformation of particles.[33] The plastic stiffness of granules also affects their compression behavior.[34] The compressibility descriptors given by the representative compressibility parameters, compressibility analysis, Walker equation, and rearrangement index of Kawakita analysis have a linear relationship with the formulation of the binary mixture.[35] Heckel evaluated the plastic deformability of powder beds by focusing on the relationship between relative density and compression pressure.[36] Heckel's analysis is the most popular method for evaluating the plasticity of powders.[37,38] Thus, despite the effect of the mixing fraction of the powder on the compression behavior, it was insufficient to predict the mixing fraction to obtain the required tablet strength.

Therefore, the purpose of this study was to quantitatively evaluate the relationship between the compression and tabletability properties of powders composed of different materials, with a particular focus on the particle plastic deformability. The compression properties of the powder mixtures of different materials with different plastic deformabilities were evaluated based on the force–displacement (F–d) curves obtained through powder compression tests. Heckel and compression energy analyses were performed to evaluate compression properties. In addition, the quantitative relationship between the compression properties and tensile strength of the compacts was investigated. Finally, a prediction equation is proposed for the compressibility of mixed powders based on the obtained relationship and the compression properties of a single material.

Experimental

Powders Microcrystalline cellulose (MCC; CEOLUS® PH-101, Asahi Kasei Corp., Japan), ascorbic acid (Asc; L-ascorbic acid, Fuso Chemical Co., Ltd., Japan), acetaminophen (AAP; ACETAMINOPHEN, BASF Japan Ltd., Japan), lactose (Lac; Dylactoze® S, FREUND Corp., Japan), and ibuprofen (IBN; IBUPROFEN, BASF Japan Ltd., Japan) were used. MCC, Lac, and Asc were sieved to sharpen their size distributions, whereas IBN and AAP could not be sieved because of their cohesiveness. The size distributions of the powders were measured under dry conditions using a laser diffraction particle size analyzer (SALD-2100, SHIMADZU Corp., Japan). The size distribution of powders was shown in Fig. 1. The properties of the powder are listed in Table 1. ρ_{true} and D_{50} were the true density and median diameter of the particles, respectively. The particle plasticity λ_{p} was defined based on the Edinburgh elastoplastic adhesion model for discrete element method as follows:
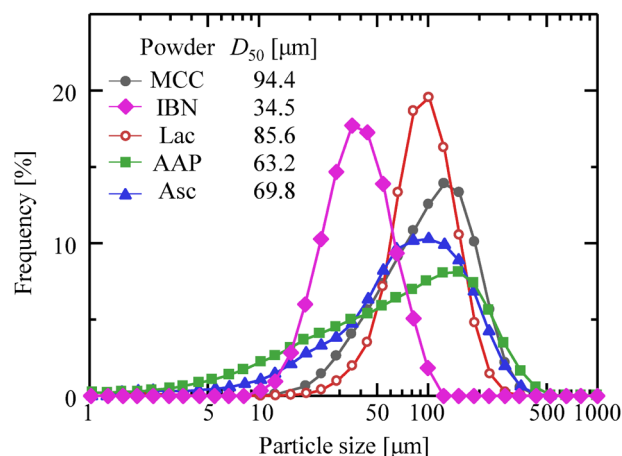
Fig. 1. Particle Size Distributions of Powders

Table 1. Properties of the Powders Used in the Study

	MCC	IBN	Lac	AAP	Asc
λ_{p} [—]	0.75[39]	0.46[40]	0.72[40]	0.66[41]	0.16[40]
ρ_{true} [kg/m³]	1566	1118	1555	1263	1694
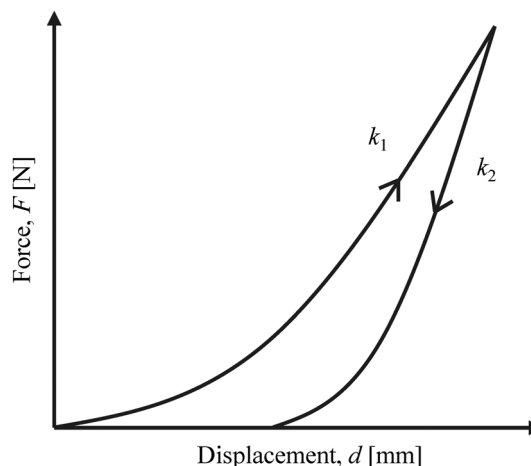
Fig. 2. Force Curve of Powder Compression to Define k_1 and k_2

$$\lambda_{\text{p}} = 1 - \frac{k_1}{k_2} \tag{1}$$

where k_1 and k_2 denote the slopes of the compression and decompression curves, respectively, as shown in Fig. 2. A material with $\lambda_{\text{p}} = 0$ is regarded as perfectly elastic. As the value of λ_{p} approaches 1, the material shows high plastic behavior. k_1 and k_2 were obtained from the nanoindentation results.

Two different powders were mixed in a mortar and pestle with different mass fractions of plastic powder (W_{p}) as follows:

$$W_{\text{p}} = \frac{m_{\text{p}}}{m_{\text{total}}} \tag{2}$$

where m_{total} and m_{p} are the total mass and mass of plastic powder, respectively. W_{p} ranged between 0 and 1.0. When MCC was used as the plastic powder, Asc, AAP, Lac, or IBN was used as the elastic powder. When Asc with the lowest λ_{p} was used as the elastic powder, Lac or IBN was used as the plastic
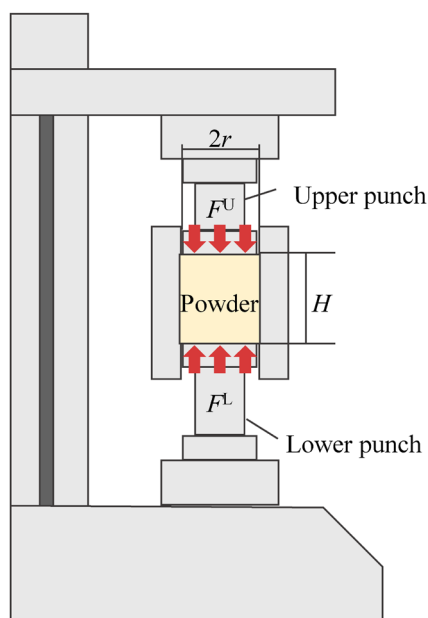
Fig. 3. Schematic of Powder Compression Tester

Fig. 4. Heckel Plot of MCC to Define the Powder Plastic Deformation K

Fig. 5. Schematic of the Compression Energy Analysis from F–d Curve

powder. Finally, the mixed powders of MCC-Asc, MCC-AAP, MCC-Lac, MCC-IBN, Lac-Asc, and IBN-Asc were prepared.

Powder Compression Test Figure 3 shows the powder compression tester (PCM-500, DARTON Corp., Japan) used in this study. It consists of a stepping motor, displacement sensor, upper punch, lower punch, die, and a measurement system for data collection. The inner diameter of die ($2r$) was 8.0 mm. After 0.2 g of powder was put into the die, the powder was compressed by moving the upper punch. Changes in the upper punch force (F^U), lower punch force (F^L), and powder bed height (H) were continuously measured during the compression, pressure relaxation, and decompression processes. The compression and decompression speeds were set to 0.1 mm/s. The height of the powder bed was corrected considering the equipment strain measured from the force curve without powder. For each powder mixture, five compression tests were performed.

Evaluation Methods

Heckel Analysis Heckel evaluated the plastic deformability of powder beds using Eq. 3 focusing on the relationship between the relative density at a certain time (ρ_{rel}) and the compression pressure (P).[36)]

$$\ln \frac{1}{1-\rho_{rel}} = KP + \ln \frac{1}{1-\rho_{rel,filling}} \tag{3}$$

$$\rho_{rel} = \frac{m_{total}}{\pi r^2 H} \tag{4}$$

Here, $\rho_{rel,filling}$, K, and r are the relative density at filling, the unique constant value of powder, and the radius of the tablet, respectively. Figure 4 shows the Heckel plot of the MCC, where the curved area **I** represents the particle rearrangement, and the linear area **II** represents the powder densification due to the plastic deformation of the particles.[42)] The value of K is correlated with the inverse of the yield stress. A higher K indicates that the powder yields easily or that it is easily plastically deformed. Therefore, in this study, we evaluated the
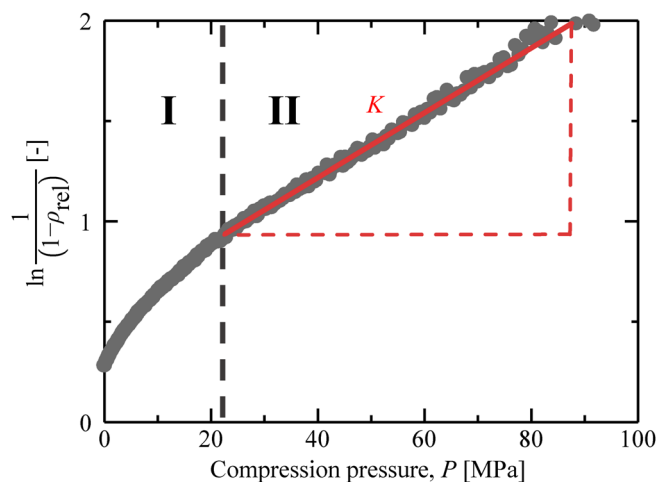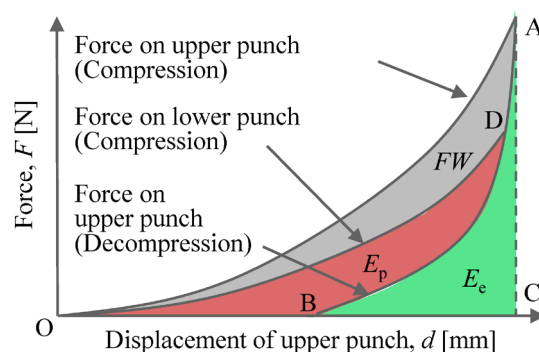
slope K of area **II** as the plastic deformability of the powder.

Energy Analysis of Powder Compression A prediction method was proposed for the capping tendency based on the ratio of elastic to plastic energy obtained from compression energy analysis.[43)] Figure 5 shows a schematic of the compression energy analysis of F–d curve. The curves OA and OD represent the compression curves of the upper and lower punches, respectively. Curve AB represents the force curve of the upper punch during decompression. The total energy of the powder compression was divided into the elastic deformation energy, plastic deformation energy, and the frictional work of the powder. The ACBDA area (green area) represents the elastic recovery energy (E_e). The OADO area (grey area) represents the loss of pressure transfer between the upper and lower punches, which was regarded as the frictional work (FW). The remaining area OBDO (red area) represents the plastic deformation energy (E_p). The ratio of the plastic to elastic energy (E_p/E_e) was calculated to evaluate the plastic deformability of the powder bed.

Tensile Strengths of the Tablets The tensile strengths of the tablets obtained from the powder compression test were evaluated using a tablet-breaking hardness tester (TH-203MP, Toyama Sangyo Co., Ltd., Japan). Force was applied in the radial direction of the tablet, and the force required to break the tablet (F_b) was measured to calculate the tensile strength (σ_d) from Eq. 5.

$$\sigma_d = \frac{F_b}{\pi r T} \quad (5)$$

where T is the tablet thickness.

This study investigated the relationship between the plastic deformability of a mixed powder and the tensile strength of a tablet.

Results and Discussion

Plastic Deformability of Elastic and Plastic Powder Mixtures The plastic deformabilities of the elastoplastic powder mixtures were evaluated using Heckel and compression energy analyses. Figure 6 shows the relationship between the mass fraction of the plastic particles (W_p) and the value of K calculated from the Heckel plot. The left and right ends of the graph show the value of K of the raw powders of elastic and plastic materials, respectively. The value of K increased in the following order: $Asc < Lac < AAP < IBN < MCC$. The order was not similar to the trend for λ_p listed in Table 1. The result indicated that λ_p, which is the plastic deformability of particles, do not always express the plastic deformability of powder. Furthermore, the plastic deformability of the powder was affected by other particle properties such as particle size. Overall, K increased with increasing W_p. The value of K increased significantly, especially when MCC was used as the plastic powder, owing to the greatest plastic deformability of MCC among those of all the powders. In contrast, the IBN-Asc and Lac-Asc conditions indicated a small change in K. This small effect of mixing occurred because the value of K of Asc was similar to those of the two powders.

E_p/E_e was calculated from the F–d curves of the powder mixtures. Figure 7 shows the relationship between E_p/E_e and W_p. The order of the E_p/E_e was $Asc < AAP < Lac < IBN < MCC$, similar to the trend observed for K. The overall trend was a nonlinear increase in E_p/E_e with W_p, whereas K increased linearly with W_p. In particular, linearity was low when Asc was the elastic material. As the compression energy analysis included the particle rearrangement process, this nonlinear behavior could be attributed to the effect of powder flowability. When the powder flowability was low, the packing structure became loose. Particle rearrangement actively occurred in the loose packing structure. The deformation of the powder due to rearrangement was not recovered by decompression. Therefore, the deformation of powder layer caused by rearrangement was considered as plastic deformation energy in the compression energy analysis. When the plastic deformability of the particle was large, the influence of the plastic deformability of the particles on E_p/E_e was significant. However, when the plastic deformability of the powder layer was small, the influence of the rearrangement on E_p/E_e was large. From the above, the linearity of the change of E_p/E_e in the case of MCC used as the plastic material increased compared to that of Asc used as the elastic material, owing to the plastic deformability of the particles.

Thus, the plastic deformability of the raw powder affected that of the two-component powder mixture. Furthermore, the large difference in plastic deformability resulted in a remarkable influence.

Relationship between Powder Plastic Deformability and Tensile Strength Figure 8 shows the relationship of σ_d with K and E_p/E_e of the elastoplastic mixtures of powders. Both
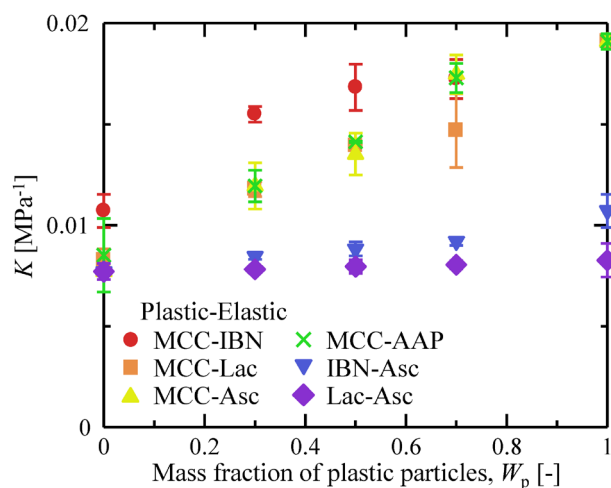
Fig. 6. Relationship between the Mass Fraction of Plastic Powders W_p and Values of K
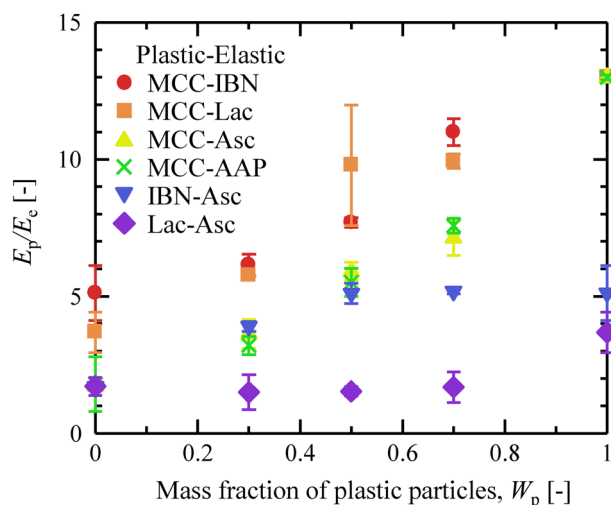
Fig. 7. Relationship between the Mass Fraction of Plastic Powders W_p and E_p/E_e

plastic deformability (K and E_p/E_e) were highly correlated with the tensile strength. As mentioned in many reports, high plastic deformability resulted in the high tensile strength of the tablet. The coefficient of determination (R^2) of E_p/E_e (0.88) was smaller than that of K (0.90) because E_p/E_e included the particle rearrangement process. The relatively high correlation observed in this study could be attributed to the use of powders of similar sizes and densities. Further investigation is necessary when materials with significantly different properties are used. In summary, the prediction of the tensile strength of tablets using these different evaluation methods should be improved. Therefore, because both evaluation methods were highly correlated with the tensile strength to some extent, a combination of the two indicators may be used to provide highly accurate predictions.

Since there was a linear relationship between K and E_p/E_e and σ_d, it was assumed that there was also a linear relationship between the combined plastic deformation parameter and σ_d. The product of powers of the variables was used as the composite plastic deformation parameter, as in the dimensionless parameters of the dimensional analysis. σ_d was described
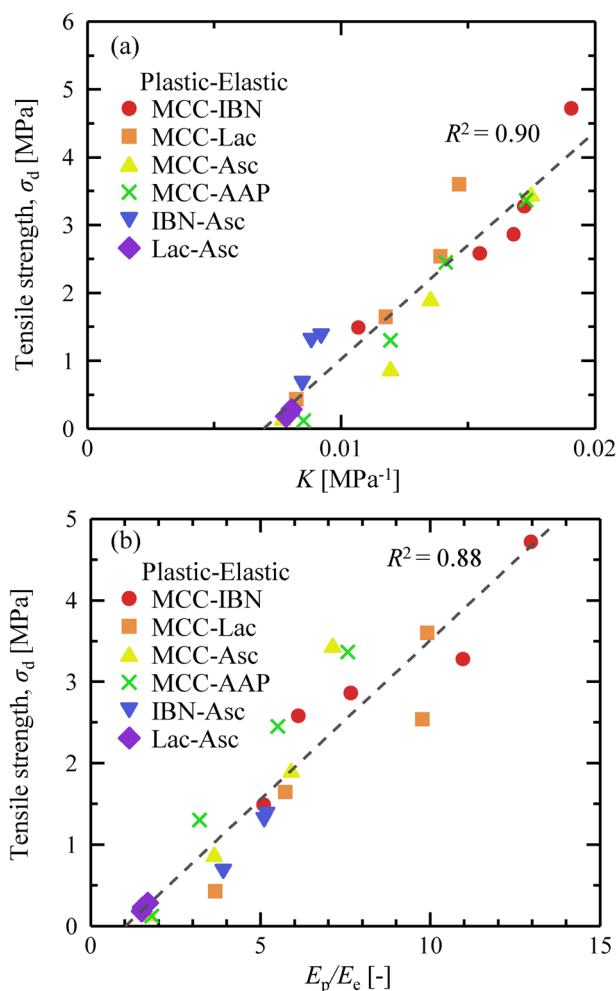
Fig. 8. Relationship of the Tensile Strength of the Tablet σ_d with (a) K and (b) E_p/E_e of the Elastoplastic Mixtures of Powders

Fig. 9. Relationship between the Experimentally Obtained and Calculated Tensile Strength Values $\sigma_{d,exp}$ and $\sigma_{d,cal}$, Respectively
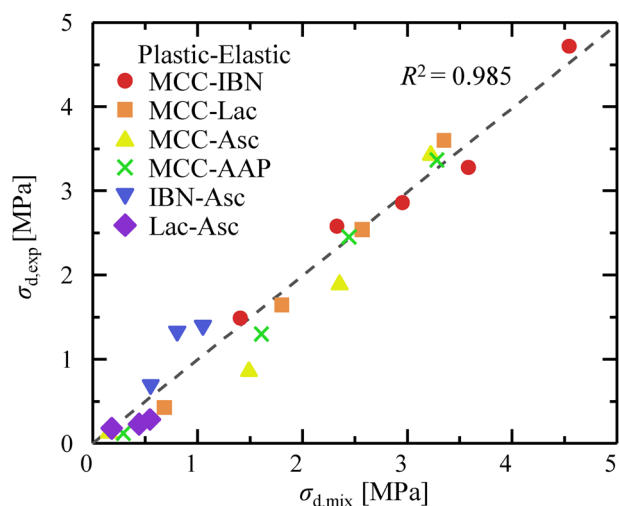
Fig. 10. The Relationship between $\sigma_{d,mix}$ and $\sigma_{d,exp}$

using E_p/E_e and K as Eq. 6. The coefficients a_1, a_2, a_3, and a_4 were appropriately determined to obtain a straight line between the measured σ_d and $f(E_p/E_e, K)$ by the least squares method. The resulting prediction equations are expressed in Eq. 7, which relates tensile strength to the plastic deformability of the powder. The exponent E_p/E_e was smaller than K but larger than 0; hence, it could not be neglected.

$$\sigma_d = a_1(E_p/E_e)^{a_2}(K)^{a_3} + a_4 \qquad (6)$$

$$\sigma_d = 50.61(E_p/E_e)^{0.355}(K)^{0.777} - 1.242 \qquad (7)$$

Figure 9 shows the relationship between the tensile strength obtained from experiments ($\sigma_{d,exp}$) and calculation ($\sigma_{d,cal}$) using Eqs. 6 and 7. The coefficient of determination was 0.986, which was higher than those for E_p/E_e or K. The combination of E_p/E_e and K demonstrated the relationship between the plastic deformability and tensile strength of the mixed powders with high accuracy.

Prediction of the tensile strength of the tablets composed of elastic and plastic powder mixtures

Using Eq. 7, the tensile strength of the tablets can be predicted once E_p/E_e and K values of the mixed powder are predicted from the compression properties of the raw powder. In this study, we assumed that E_p/E_e and K of the mixed powder

could be calculated from the relationship between the plastic deformability of the raw powder and W_p as shown in Eqs. 8 and 9.

$$(E_p/E_e)_{mix} = (E_p/E_e)_p \times W_p + (E_p/E_e)_e \times (1 - W_p) \qquad (8)$$

$$K_{mix} = K_p \times W_p + K_e \times (1 - W_p) \qquad (9)$$

The subscripts mix, p, and e indicate mixed powder, plastic particles, and elastic particles, respectively. Figure 10 shows the relationship between the experimental and calculated tensile strength values obtained by substituting $(E_p/E_e)_{mix}$ and K_{mix} into Eq. 7. Because the correlation coefficient exceeded 0.9, the assumptions in Eqs. 8 and 9 could be applied. Table 2 lists the coefficient of determination. The calculated values under the conditions using MCC as a plastic material had a good agreement with the experimental values since the coefficients of determination were over 0.95. In contrast, the coefficients of determination using Asc as an elastic material was quite low, owing to small tablet strength. Since tensile strength of the tablets under the conditions in which Asc

Table 2. Coefficients of Determination under the Conditions Using Different Powder Mixtures

Powder	Coefficient of determination
MCC:IBN	0.963
MCC:Lac	0.983
MCC:Asc	0.951
MCC:AAP	0.988
IBN:Asc	0.688
Lac:Asc	−3.312
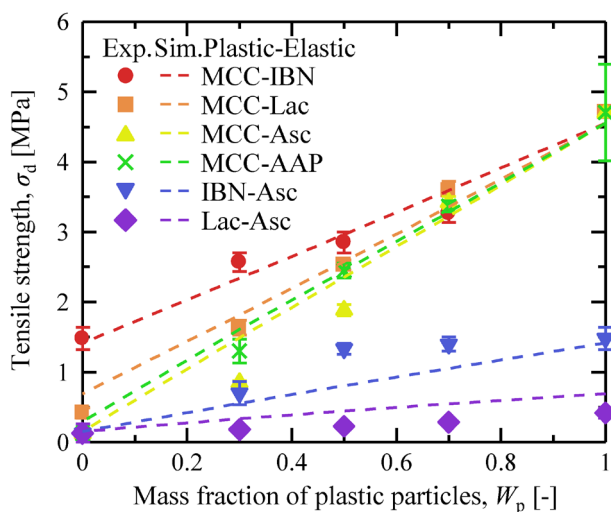
Fig. 11. Comparison between the Experimental Tensile Strength and Predicted Lines as a Function of the Mass Fraction of Plastic Powders for Different Powder Mixtures

was used as the elastic material was extremely small, tablet strength prediction was not necessary for practical purposes. The results indicated that the plastic deformability of mixed powders can be predicted based on the plastic deformability of a single material.

Finally, the tensile strength of the mixed powder was predicted using $\sigma_{d,mix}$ and W_p. Figure 11 shows the experimental and predicted tensile strengths as functions of the plastic powder mass fraction for different powder mixtures. Although the predicted lines when using Asc as the elastic material indicated values different from the experimental values, the predicted lines when using MCC as the plastic material concurred well with the experimental ones. Thus, the tensile strength of a powder mixture can be predicted based on the compression properties of a single-component powder material when a highly plastic material is used. The obtained findings suggested that the mass fraction of the powder mixture had a significant effect on tensile strength. The tablets in actual industry often contain tiny amount of a lubricant. The prediction equation in this study should be applicable even when a lubricant is added because the mass of a lubricant is small.

This result provides a quantitative indicator of the ideal mass fraction for forming a tablet with sufficient strength composed of a mixture with different plastic deformabilities.

Conclusion

The compression properties of the powder mixtures with different plastic deformabilities were evaluated. When particles of high plastic deformability were used, the plastic deformability of the powder was also high. A correlation equation was proposed for the tablet strength by combining K and E_p/E_e obtained from the Heckel and compression energy analyses, respectively. Furthermore, by substituting the compression properties of a single material and mass fraction into the proposed equation, the tablet strength of a powder mixture with different plastic deformabilities when using a highly plastic material was predicted. This prediction equation enables the easy determination of the mass fraction required to produce tablets with the required tensile strength from the powder properties of a single material.

Conflict of Interest The authors declare no conflict of interest.

References

1) Yu Y., Zhao L., Lin X., Wang Y., Feng Y., *Int. J. Pharm.*, **577**, 119023 (2020).
2) Liu F., Zhang J., Liu P., Deng Q., He D., *Ceram. Int.*, **46**, 3984–3988 (2020).
3) Bai Y., Li L., Fu L., Wang Q., *Sci. Prog.*, **104**, 1–20 (2021).
4) Guo J., Zhao X., Herisson De Beauvoir T., Seo J. H., Berbano S. S., Baker A. L., Azina C., Randall C. A., *Adv. Funct. Mater.*, **28**, 1–15 (2018).
5) Aziz M. G., Yusof Y. A., Blanchard C., Saifullah M., Farahnaky A., Scheiling G., *Food Eng. Rev.*, **10**, 66–80 (2018).
6) Sakuda A., Hayashi A., Tatsumisago M., *Sci. Rep.*, **3**, 2261 (2013).
7) Parafiniuk P., Molenda M., Horabik J., *Physica A*, **416**, 279–289 (2014).
8) Deng X. L., Davé R. N., *Granul. Matter*, **15**, 401–415 (2013).
9) Chandler H. W., Sands C. M., Song J. H., Withers P. J., McDonald S. A., *Int. J. Solids Struct.*, **45**, 2056–2076 (2008).
10) Okada N., Hayashi Y., Onuki Y., Miura T., Obata Y., Takayama K., *Chem. Pharm. Bull.*, **64**, 1142–1148 (2016).
11) Hayashi Y., Okada N., Takayama K., Obata Y., Onuki Y., *Chem. Pharm. Bull.*, **66**, 727–731 (2018).
12) Yokota M., Kusano T., Mori M., Okuda K., Matsunaga T., *Powder Technol.*, **380**, 265–272 (2021).
13) Meynard J., Amado-Becker F., Tchoreloff P., Mazel V., *Int. J. Pharm.*, **621**, 121818 (2022).
14) Uzondu B., Leung L. Y., Mao C., Yang C. Y., *Int. J. Pharm.*, **543**, 234–244 (2018).
15) Sun C. C., *Powder Technol.*, **279**, 123–126 (2015).
16) Wu C. Y., Ruddy O. M., Bentham A. C., Hancock B. C., Best S. M., Elliott J. A., *Powder Technol.*, **152**, 107–117 (2005).
17) Inghelbrecht S., Remon J. P., *Int. J. Pharm.*, **161**, 215–224 (1998).
18) Shi Z., Liu S., *Eur. J. Oper. Res.*, **287**, 133–144 (2020).
19) Persson A. S., Alderborn G., *Eur. J. Pharm. Biopharm.*, **125**, 28–37 (2018).
20) Nakamura H., Sugino Y., Iwasaki T., Watano S., *Chem. Pharm. Bull.*, **59**, 1518–1522 (2011).
21) Takeuchi H., Nagira S., Yamamoto H., Kawashima Y., *Int. J. Pharm.*, **274**, 131–138 (2004).
22) Imayoshi Y., Ohsaki S., Nakamura H., Watano S., *Chem. Pharm. Bull.*, **71**, 566–575 (2023).
23) Duberg M., Nyström C., *Powder Technol.*, **46**, 67–75 (1986).

24) Portnikov D., Kalman H., *Powder Technol.*, **268**, 244–252 (2014).
25) Fedotov A. F., *Powder Metall. Met. Ceramics*, **50**, 301–312 (2011).
26) Roberts R. J., Rowe R. C., *Int. J. Pharm.*, **36**, 205–209 (1987).
27) Jain S., *Pharm. Sci. Technol. Today*, **2**, 20–31 (1999).
28) Martin C. L., Bouvard D., *Acta Mater.*, **51**, 373–386 (2003).
29) Strege S., Weuster A., Zetzener H., Brendel L., Kwade A., Wolf D. E., *Granul. Matter*, **16**, 401–409 (2014).
30) Shah U. V., Karde V., Ghoroi C., Heng J. Y. Y., *Int. J. Pharm.*, **518**, 138–154 (2017).
31) Penkavova V., Kulaviak L., Ruzicka M. C., Puncochar M., Grof Z., Stepanek F., Schongut M., Zamostny P., *Powder Technol.*, **342**, 887–898 (2019).
32) De Pue J., Di Emidio G., Verastegui Flores R. D., Bezuijen A., Cornelis W. M., *Soil Tillage Res.*, **194**, 104303 (2019).
33) Biswas K., *J. Mater. Process. Technol.*, **166**, 107–115 (2005).
34) Tofiq M., Nordström J., Persson A. S., Alderborn G., *Powder Technol.*, **399**, 117207 (2022).
35) Berkenkemper S., Klinken S., Kleinebudde P., *Powder Technol.*, **424**, 118571 (2023).
36) Heckel R., *Trans. Metal. Soc. of AIME*, **221**, 671–675 (1961).
37) Paul S., Sun C. C., *Int. J. Pharm.*, **532**, 124–130 (2017).
38) Ilkka J., Paronen P., *Int. J. Pharm.*, **94**, 181–187 (1993).
39) Das K., Ray D., Bandyopadhyay N. R., Sengupta S., *J. Polym. Environ.*, **18**, 355–363 (2010).
40) Masterson V. M., Cao X., *Int. J. Pharm.*, **362**, 163–171 (2008).
41) Liao X., Wiedmann T. S., *J. Pharm. Sci.*, **93**, 2250–2258 (2004).
42) Ghori M. U., *Br. J. Pharm.*, **1**, 19–29 (2016).
43) Nakamura H., Sugino Y., Iwasaki T., Watano S., *Chem. Pharm. Bull.*, **59**, 1518–1522 (2011).